AD-A141 410 INTERACTIONS BETWEEN EROSION AND CORROSION OF METALS AND ALLOYS AT ELEVAT..(U) PITTSBURGH UNIV PA DEPT OF METALLURGICAL AND MATERIALS ENGINE.. N BIRKS ET AL. 1/

UNCLASSIFIED APR 84 ARO-17421.1-MS DAAG29-81-K-0027 F/G 11/6 NL

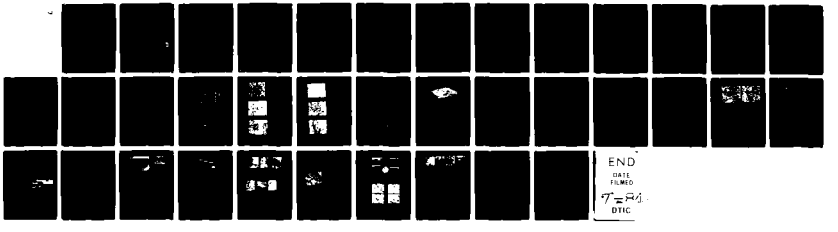

END
DATE FILMED
7-84
DTIC

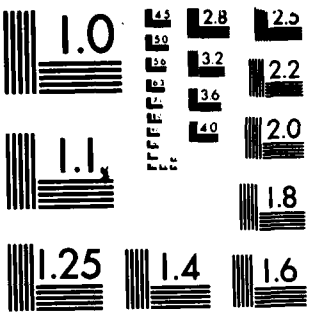

Unclassified

SECURITY CLASSIFICATION OF THIS PAGE (When Data Entered)

REPORT DOCUMENTATION PAGE

READ INSTRUCTIONS BEFORE COMPLETING FORM

1. REPORT NUMBER: ARO 17421.1-MS
2. GOVT ACCESSION NO.:
3. RECIPIENT'S CATALOG NUMBER:

4. TITLE (and Subtitle): Interactions Between Erosion and Corrosion of Metals and Alloys at Elevated Temperatures

5. TYPE OF REPORT & PERIOD COVERED: Final Report 5 Jan 81 - 4 Jan 84

6. PERFORMING ORG. REPORT NUMBER:

7. AUTHOR(s): N. Birks and F. S. Pettit

8. CONTRACT OR GRANT NUMBER(s): DAAG29-81-K-0027

9. PERFORMING ORGANIZATION NAME AND ADDRESS: Pittsburgh, Univ

10. PROGRAM ELEMENT, PROJECT, TASK AREA & WORK UNIT NUMBERS: N/A

11. CONTROLLING OFFICE NAME AND ADDRESS: U. S. Army Research Office, Post Office Box 12211, Research Triangle Park, NC 27709

12. REPORT DATE:

13. NUMBER OF PAGES:

14. MONITORING AGENCY NAME & ADDRESS (if different from Controlling Office):

15. SECURITY CLASS. (of this report): Unclassified

15a. DECLASSIFICATION/DOWNGRADING SCHEDULE:

16. DISTRIBUTION STATEMENT (of this Report): Approved for public release; distribution unlimited.

17. DISTRIBUTION STATEMENT (of the abstract entered in Block 20, if different from Report):

18. SUPPLEMENTARY NOTES: The view, opinions, and/or findings contained in this report are those of the author(s) and should not be construed as an official Department of the Army position, policy, or decision, unless so designated by other documentation

19. KEY WORDS (Continue on reverse side if necessary and identify by block number):
High Temperature
Erosion
Corrosion
Metallic
Alloys

20. Structural alloys and coating alloys have been developed that successfully resist high temperature oxidation and, to a lesser extent, hot corrosion-depending on conditions. Such protection depends upon the maintenance of a surface layer of oxide that effectively separates the metal from the reactive environment.

DD FORM 1 JAN 73 1473 EDITION OF 1 NOV 65 IS OBSOLETE

UNCLASSIFIED

ARO 17421.1-MA
20. ABSTRACT CONTINUED:

The oxide protective coatings may however be damaged by erosion by solid particles in the gas flow, the effect being worse when the velocity of the gas flow is high. Unfortunately the detailed mechanisms by which the processes of erosion and oxidation interact at high temperatures are not understood. Much of the work carried out so far has involved studies of the erosion of metals and oxidized metals at room temperature under controlled conditions, or has involved tests at hightemperature under conditions designed to simulate those in gas turbines or coal combustors. The data obtained from such tests are well suited to producing reliable comparisons of the behavior of different materials but do not readily lead to analysis of the mechanisms by which erosion and corrosion interact at high temperature.

The work described in this report was designed to provide data obtained under well characterized conditions such that understanding could be gained concerning the interaction of erosion and corrosion at high temperatures.

ARO 17421.1-MS

Interactions Between Erosion and Corrosion of Metals and Alloys at Elevated Temperatures

Prepared by
N. Birks and F. S. Pettit

Final Report April 1984

prepared for
U.S. Army Research Office
Research Triangle Park
North Carolina 27709

Project Number 0-17421-MS
Contract Number: DAAG 29-81-K-0027

University of Pittsburgh
Metallurgical and Materials Engineering Dept.
Pittsburgh, PA 15261

April 1984

CONTENTS

ITEM	PAGE
Forward	1
Statement of Problem	1
Design and Construction of Apparatus	2
Main Results Obtained and their Significance	3
(a) Morphological Features	3
(b) Measurement and Interpretation of Reaction Rates	6
Accomplishments	8
List of Illustrations	10
Participating Scientific Personnel	11
Appendix - Published Paper	11

INTERACTIONS BETWEEN EROSION AND CORROSION OF METALS AND ALLOYS AT ELEVATED TEMPERATURES

Forward

Structural alloys and coating alloys have been developed that successfully resist high temperature oxidation and, to a lesser extent, hot corrosion-depending on conditions. Such protection depends upon the maintenance of a surface layer of oxide that effectively separates the metal from the reactive environment.

The oxide protective coatings may however be damaged by erosion by solid particles in the gas flow, the effect being worse when the velocity of the gas flow is high. Unfortunately the detailed mechanisms by which the processes of erosion and oxidation interact at high temperatures are not understood. Much of the work carried out so far has involved studies of the erosion of metals and oxidized metals at room temperature under controlled conditions, or has involved tests at hightemperature under conditions designed to simulate those in gas turbines or coal combustors. The data obtained from such tests are well suited to producing reliable comparisons of the behavior of different materials but do not readily lead to analysis of the mechanisms by which erosion and corrosion interact at high temperature.

The work described in this report was designed to provide data obtained under well characterized conditions such that understanding could be gained concerning the interaction of erosion and corrosion at high temperatures.

Statement of the Problem

The problem to be studied was resolved into two distinct parts. Firstly it was necessary to design, construct and test an apparatus in which specimens could be exposed under controlled conditions. Secondly the apparatus was to be used to study the erosion-corrosion interactions associated with the exposure of nickel and cobalt to these conditions.

Design and Construction of Apparatus

The design aims were as follows:

(a) To deliver a gas flow at speeds up to 300 ms^{-1}, calibrated at temperatures up to 900°C

(b) To introduce solid particles to the gas stream in metered quantities, to heat them to design temperature and accelerate them to design velocity.

(c) To design a specimen holder allowing easily reproducible positioning of the sample that can be heated

(d) To obtain measurements of the kinetics of the process.

All of these aims have been achieved as classified below, the schematic layout of the apparatus is given in Figure 1.

(a) The gas is heated by in line gas flow heaters and then passed down a vertical, 1.5m long, aluminized inconel tube of 8mm diameter inside a series of heating furnaces. Using this system, the gas flow can be heated to 900°C and 100 ms^{-1} and to 800°C at higher velocities.

(b) Solid particles are introduced to the gas stream from a Sylco particle dispenser at the top of the inconel tube. A gas flow divider is used to reduce the particle loading to levels below that normally obtained using the Sylco dispenser. The speed of the particles leaving the 1.5m inconel tube was measured using the laser doppler velocimeter and found to agree well with calculated values. This equipment also gives data yielding a complete frequency distribution of particle speeds. The laser velocimeter may be used in hot or cold gas streams, in situ, without disturbing the apparatus.

(c) A specimen holder locks the specimen on three points and is spring loaded to prevent loosening due to expansion as the temperature is increased. The holder is mounted on a swivel and can be positioned reliably and rapidly in the gas stream. Mainly, the specimen is heated by the hot gas stream, supplementary heating from below using a radiant focussing heater is used to eliminate temperature gradients. The specimen can be held in the holder at selected angles to the erosive stream.

(d) The rates of simultaneous attack by erosion and corrosion cannot be measured in the usual way since the errosive component produces a loss in weight due to material removal, whereas the oxidation component results in a weight gain due to formation of oxide. Furthermore simple oxide formation will occur over that part of the specimen surface that is not undergoing erosion. This has been overcome in two ways. Firstly a thick oxide layer was formed prior to erosion such that the oxidation rate on non-eroded surfaces could be neglected. Secondly the specimens were aluminized so that negligble oxidation attack occured over the surfaces not exposed to erosion.

The initial part of the experimental period of this project was devoted to understanding the morphologies that were produced during erosion - oxidation processes.

The final part of the project was concerned with measurement also of the kinetics of the process in order to understand the mechanism of material removal.

Main Results Obtained and Their Significance

(a) Morphological Features

Initial work was concentrated on pure nickel, Ni-270, because its oxidation behavior is well characterized. Furthermore the simple NiO scale grows quite rapidly and is reasonably plastic at high temperatures.

The metal was exposed to many conditions involving a variety of speeds, temperatures, and angles of impingement. In all cases the specimens were examined using SEM-EDX techniques and an electrolytic scale stripping procedure was evolved to allow the metal and scale surfaces at the metal-scale interface to be examined.

The early work established that, starting with a polished nickel specimen, a thin (1μm) scale was formed under erosion-oxidation conditions that showed mogul (hill and valley topography) development with 90° incidence of the erosion stream, whereas the moguls were aligned into ripples at acute angles of incidence such as 45°. This scale was comprised of nickel oxide with embedded alumina particles, with clear evidence of cutting and plastic deformation of the oxide. The metal is also apparently deformed plastically under the impacts. It is thought that the plastic deformation of the metal below the scale is primarily responsible for the formation of mogul or ripple features. The particle impacts are also thought to cause extrusion of both metal and oxide, thus exposing a greater surface area of both to the atmosphere and increasing the oxidation rate.

These features involving plastic deformation and particle capture can be seen in Figures 2 and 3. A mechanism is proposed to account for the steps in the erosion oxidation of nickel is shown in Figure 4(a).

The erosion of a piece of nickel that had previously been oxidized in air to produce a thick (10μm) scale confirmed these ideas in that the central region of the scale under the erosion flux rapidly thinned down and using 90° incidence,

developed mogul formation in the surface. The outer areas of the specimen, not subject to the same intensity of erosion , did not form moguls. This confirms that these surface features are developed only when the underlying metal is being deformed plastically. The NiO of this thick scale showed the same evidence of cutting and plastic deformation as previously.

To test the role of plastic deformation of the metal in mogul formation, a model, using computer simulation, was constructed based on the formation of a well with raised rim with no material removal at each impact. The computer then summed the effects of many such impacts occurring at random over a surface. The resulting surface profile, shown in Figure 5, is very similar to the mogul pattern observed on our specimens. This confirms the role of metal plastic deformation in mogul formation and also indicates that moguls may form in the absence of material removal, i.e., they are a feature that is developed simply by rearrangement of the surface and do not require material removal for their formation.

The mechanisms by which material is removed are thought to be partly by adhesion to the erosive particles. This is shown in Figure 4 which also shows in Figure 4(b) how the thick oxide scale is reduced in thickness by erosion until interaction with the metal occurs.

Material removal by adhesion to alumina erosion particles has been confirmed by examination of such particles after impact when NiO was seen adhering to the surfaces. Approximations show that about 10% of the material removal might occur by this mechanism. An alternate mechanism might involve the cutting off of oxide protrusions produced by plastic deformation, however such pieces of NiO were not found among the post-impact particles.

The generation of a thin scale on the nickel specimens subjected to erosion oxidation conditions is regarded as reflecting the relative rates at which erosion of oxide by the alumina and formation of the oxide by oxidation can occur. It also reflects the kinetic laws followed by the two processes.

For instance, if both oxidation and erosion occurred at constant rates the rate of scale formation would be written, in terms of scale thickness (X):

$$\frac{dX}{dt} = k_o - k_e \qquad (1)$$

where ko and ke are the constant rates at which oxidation of nickel and erosion of nickel oxide occur respectively.

Clearly, from equation (1) the scale growth rate must be positive or negative and the scale thickness must increase or decrease continuously. The scale can never achieve constant thickness.

However, the oxidation rate normally follows diffusion controlled kinetics, in which case the scale thickness will change according to:

$$\frac{dX}{dt} = \frac{k}{X} - ke \qquad (2)$$

Where k is the parabolic rate constant for nickel. This will lead to the establishment of a steady state where the scale thickness remains constant at X* where dX/dt = 0 i.e. where

$$X^* = k/ke \qquad (3)$$

Although the scale thickness is constant, metal removal has not ceased, on the contrary it is being removed at a constant rate given by

$$\frac{dx}{dt} = \frac{V_M}{V_{Mo}} \frac{k}{X^*}$$

Where x is the thickness of metal removed and V_M and V_{Mo} are the molar volumes of metal and oxide respectively.

These expressions and the conditions under which they are derived are only valid where the scale is compact, regular and continuous. They will not be valid under conditions where the metal is being deformed below the scale by the erosive stream. Under these conditions new factors such as extrusion of metal and oxide are expected to lead to anomalies in oxidation behavior.

The analysis given here indicates that it is possible to obtain information on the rates of erosion from morphological examination and measurement of limiting scale thickness. The measurement of reaction kinetics however, using a direct technique was one of the aims of this program and such a technique has been developed being used in an initial stage of development during this contract period.

(b) Measurement and Interpretation of Reaction Rates

In order to obtain kinetic data it is necessary to suppress reaction on all surfaces of the sample other than that which is being exposed to erosion and corrosion. This was achieved in two ways (a) by oxidizing the nickel to produce a thick scale all over, (b) by aluminizing the specimen. In both cases the surface to be eroded could be exposed by polishing back to expose the nickel metal for testing. Corrections to the erosive weight changes due to weight gain by oxidation on the 'passivated' surfaces was low and could be calculated to provide a correction. To obtain immediate results, the preoxidizing technique was adopted.

Using this technique, data on the rates of attack by erosion-oxidation were obtained under a variety of conditions. The extent of reaction was assessed after a sample had been exposed for a given time by measuring the weight change. Figure 6 shows such data plotted for both nickel and cobalt specimens. In all cases 90° incidence of the erosive flux was used and the results in Figure 6 show the weight loss for both NiO, Ni and Co at 800°C and room temperature and at velocities of 73–80 ms^{-1} and 120 ms^{-1}.

It should be noticed that this type of data is not immediately comparable since the weight loss data for NiO, which refers to a very thick scale of NiO grown on nickel, refers to the loss of NiO by erosion, whereas a specimen of

initially polished nickel shows a weight loss that reflects loss of nickel which forms oxide. The oxide is removed as fast as it is formed, thus the weight loss measured refers to nickel only. These two conditions therefore give data that reflect differently on the extent or rate of damage caused to the metal substrate.

Tests carried out at room temperature showed that nickel and cobalt were removed only slowly and the surfaces showed evidence of substantial plastic deformation.

A nickel specimen eroded in a stream of nitrogen (to exclude air [illegible] oxidation reactions) also showed little weight change but extensive pl[illegible] deformation. In fact a slight weight gain was recorded, due to oxidation that occurred when the erosive stream was stopped at temperature. This shows that, under the conditions used, the very ductile metal is not removed very rapidly by erosion in the absence of oxidation.

The result infers that the formation of oxide is essential for the removal of nickel by erosion as NiO.

The synergistic effect of erosion and oxidation has therefore been clarified both morphologically and in terms of a detailed mechanism. Although nickel metal is not substantially removed by erosion, the less plastic nickel oxide is. The major event appears to be removal of nickel oxide by erosion, this reduces the thickness of the NiO protective layer and promotes oxidation of nickel at a high rate corresponding to the parabolic oxidation law. Thus the role of erosion is to maintain the oxide layer at small thicknesses thus ensuring that the nickel attrition occurs at high rates.

This mechanism does not hold in detail when very thin scales (1μm) are

formed since, in this case, the plastic deformation of the underlying metal results in extrusion of oxide and metal platelets which may be removed by erosive cutting, or which oxidize to NiO. This feature will ensure more rapid oxidation of the nickel and a further increase in rate of damage to the metal.

Similar results are observed in the case of cobalt, in all of the cases examined erosion occurs by a ductile mechanism, with some evidence of the oxide cracking at room temperature.

It is not possible yet to decide which erosion mechanism predominates (micromachining or platelet formation) but it is clear that the metal attrition is much greater under conditions where it may form an oxide. The observed more extensive removal of oxide by erosion is thought to be due to the fact that the ductility of the oxide is less than that metal.

Accomplishments

- An apparatus has been designed and constructed which allows a well characterized erosive stream to impinge on a specimen under closely controlled conditions.
- Particle speeds up to 240ms^{-1} and temperatures up to 900°C have been achieved.
- Particle speed and speed distribution of the particles can be measured accurately in situ, using the laser doppler velocimeter.
- A specimen may be exposed at temperatures up to 900°C and at any chosen orientation to the erosive stream.
- This apparatus is believed to be unique, no other comparable unit is known to be operating.
- A technique allowing assessment of the kinetics of the erosion-oxidation process has been developed.

- Both nickel and cobalt undergo faster material removal under conditions supporting oxide formation than in the absence of scale formation.
- The rates of erosion of nickel and cobalt oxides vary with particle velocity and temperature.
- Both metals and oxides undergo plastic deformation during erosion, the extremely ductile nature of the metal results in a low rate of removal by direct erosive action in the absence of oxide formation.
- Mogul formation is a result of very ductile behavior under impact and does not necessarily imply that material removal has occurred. This conclusion is confirmed by a statistical model.
- A mechanism is proposed to account for the more rapid attrition of the metal by conjoint oxidation and erosion in which the protective oxide scale is thinned by erosion, thus ensuring rapid oxidation.
- The main nature of the interactive process is that the erosion removes the oxide and metal is removed by forming oxide.

List of Illustrations

Figure 1. Schematic diagram of apparatus for the simultaneous erosion and oxidation of metals.

Figure 2. Ni exposed for 8 min. at 810°C at 90° to 190 ms^{-1} airflow containing 1500 ppm Al_2O_3.

Figure 3. Ni exposed for 30 min. at 730°C at 45° to 120 ms^{-1} airflow containing 2400 ppm Al_2O_3.

Figure 4. Steps in the erosion oxidation mechanism of nickel.

Figure 5. Computer simulation of surface morphology showing mogul formation after 10^6 random impacts each causing plastic deformation profile as shown, assuming that no material removal occurs.

Figure 6. Weight change with time for various erosion-oxidation conditions.

Participating Scientific Personnel

C. T. Kang: 1981-83 will shortly submit his thesis for Ph.D.
S. L. Chang: 1981-83 received M.S. in April 1984.
A. G. F. Alabi: received limited support and is currently pursuing research for Ph.D. in a different subject area.
M. Miller: received limited support, he presently holds a position in industry.

Appendix - Published Paper

"Erosion-Corrosion of Coatings and Superalloys in High Velocity Hot Gases" by C. T. Kang, S. L. Chang, N. Birks and F. S. Pettit. Proceedings JIMIS-3 (1983) p. 87. High Temperature Corrosion Transactions of the Japan Institute of Metals Supplement.

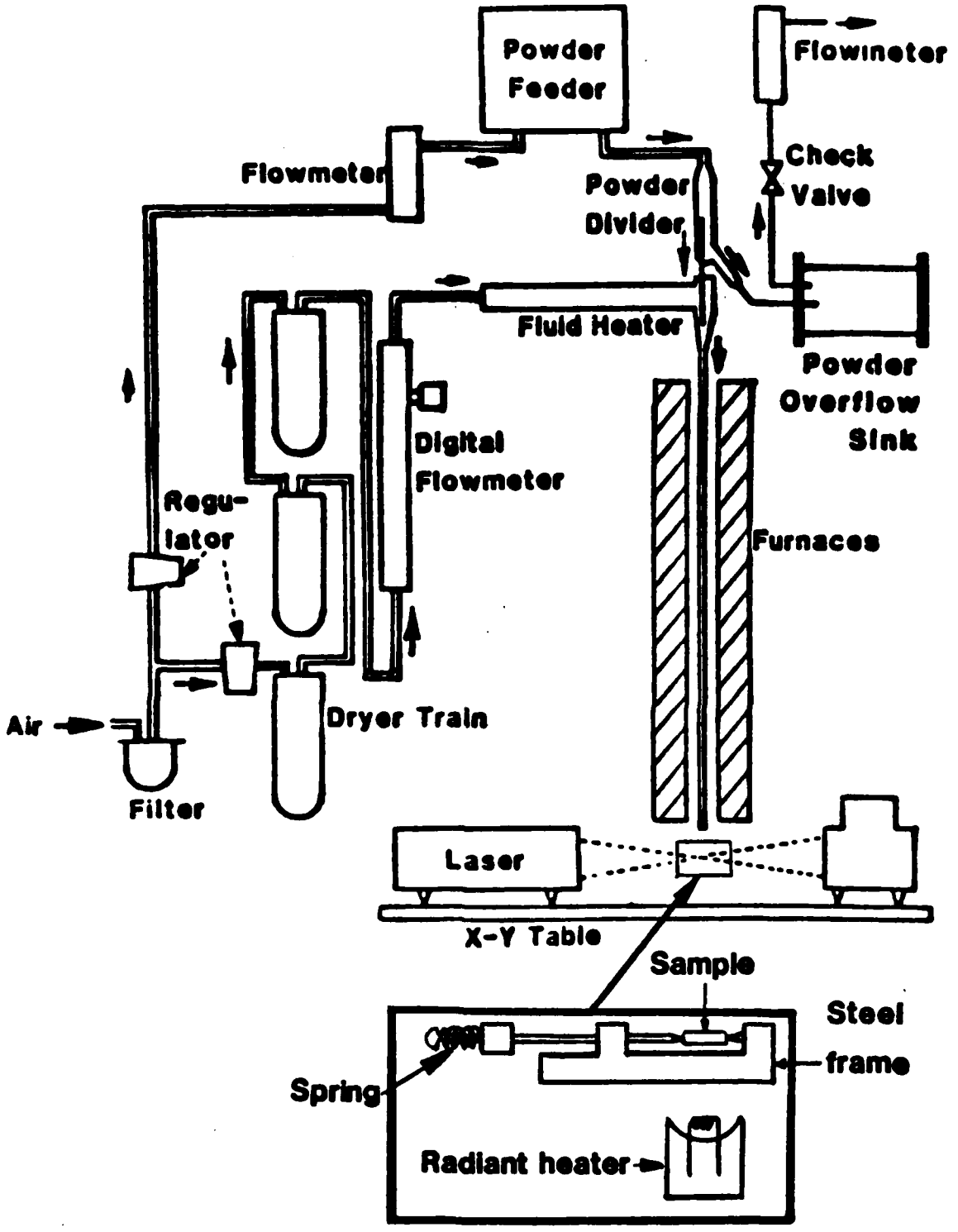

FIGURE 1 Schematic diagram of apparatus for the simultaneous erosion and oxidation of metals.

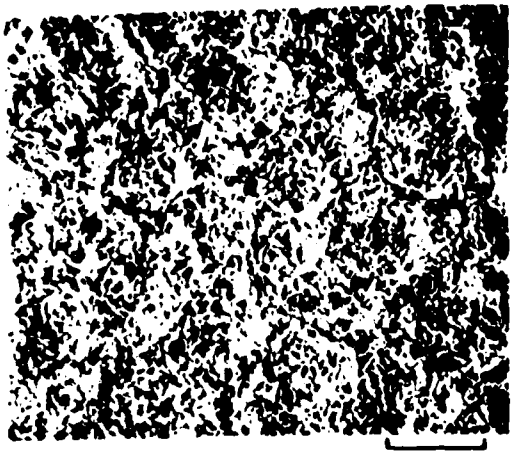

(a) oxide surface

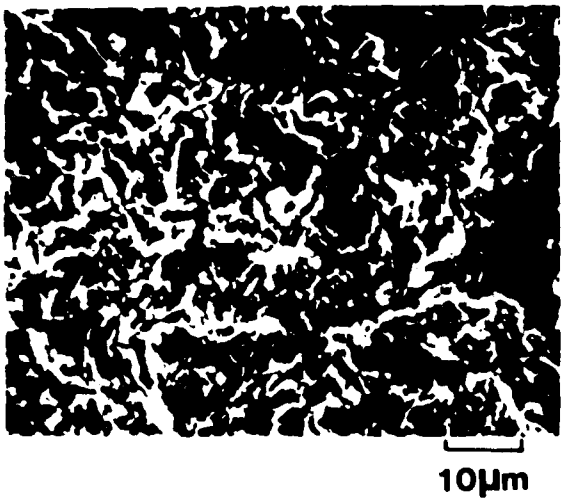

(b) oxide surface with embedded Al_2O_3 particles

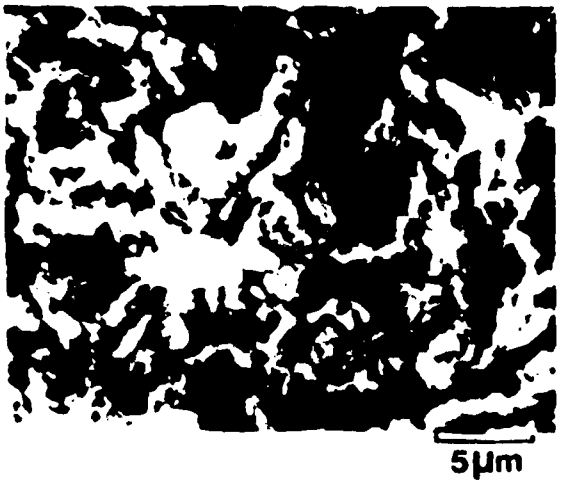

(c) as (b)

Figure 2 Ni exposed for 8 min at 810°C at 90° to 190 ms^{-1} airflow containing 1500 ppm Al_2O_3.

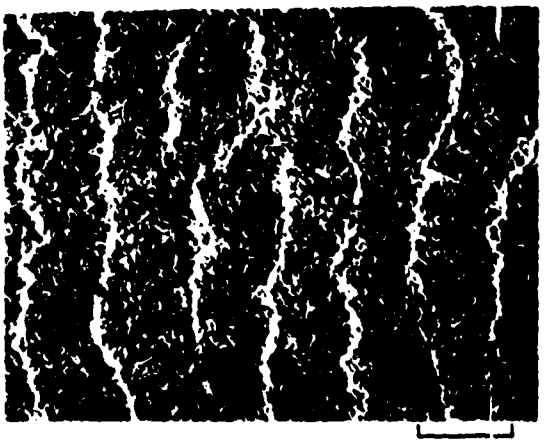

(a) oxide surface showing development of ripples

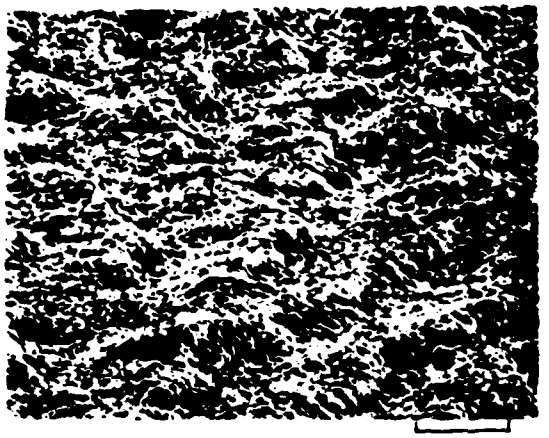

(b) oblique view of surface in (a)

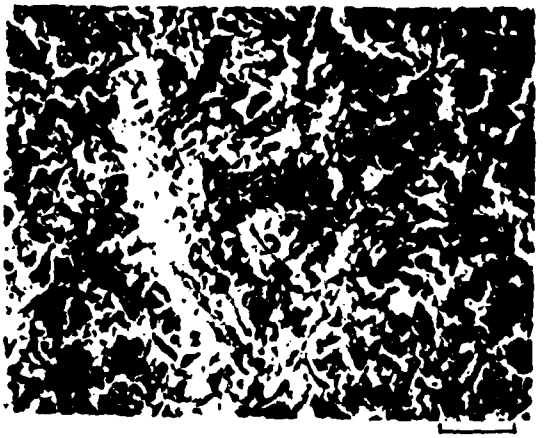

(c) specimen surface showing ripple, erosive cuts, and embedded Al_2O_3

Figure 3 Ni exposed for 30 min at 730 °C at 45° to 120 ms^{-1} airflow containing 2400 ppm Al_2O_3.

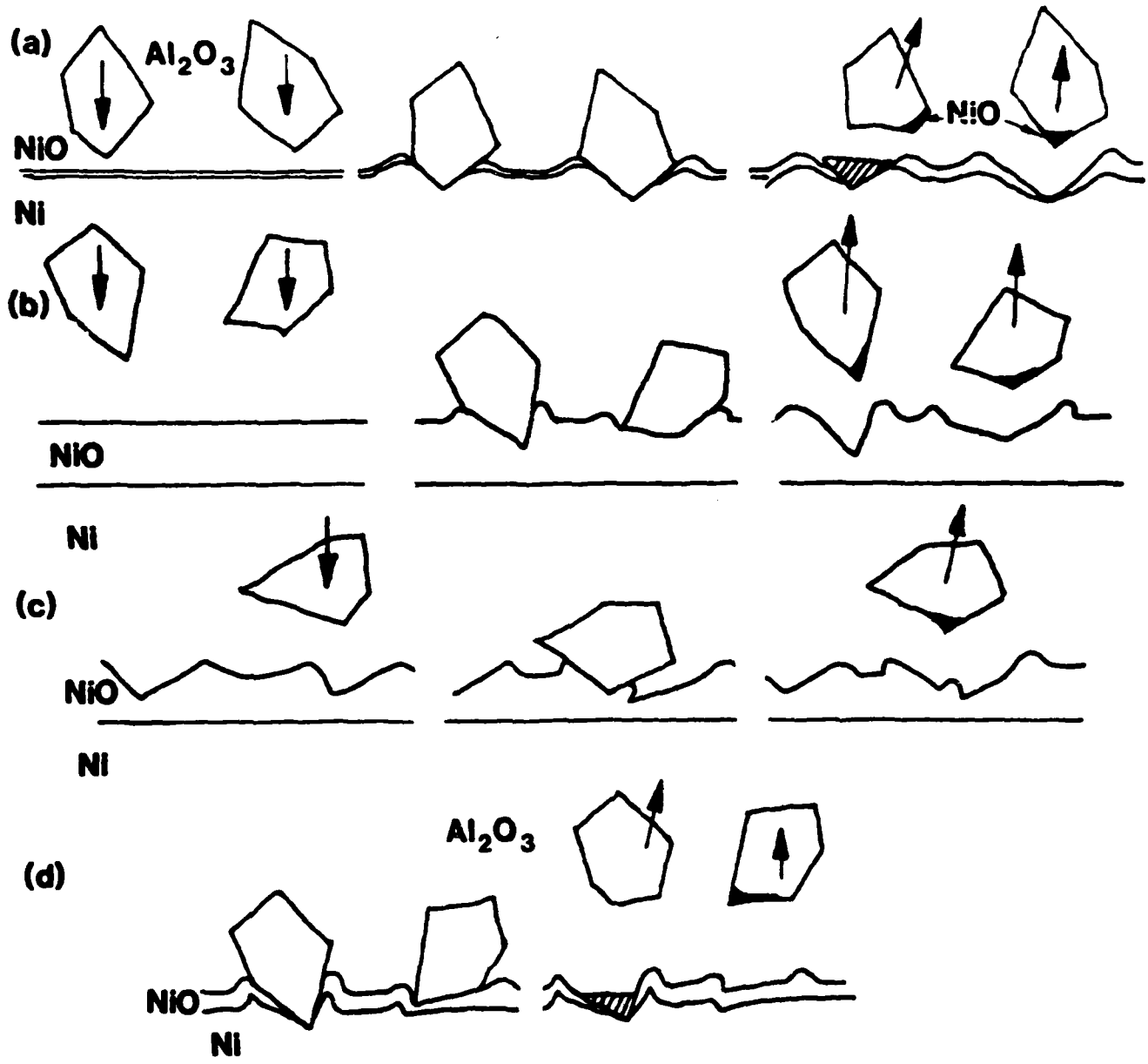

FIGURE 4 Steps in the erosion-oxidation mechanism of nickel. (a) Clean Ni surface. Al_2O_3 particles embed, both metal and oxide deform plastically on impact. (b) Ni with thick preoxidised scale. Plastic deformation of oxide only progressive thinning of scale as in (c) and (d). In (d) both metal and oxide deform plastically Al_2O_3 particles embed in metal as in (a).

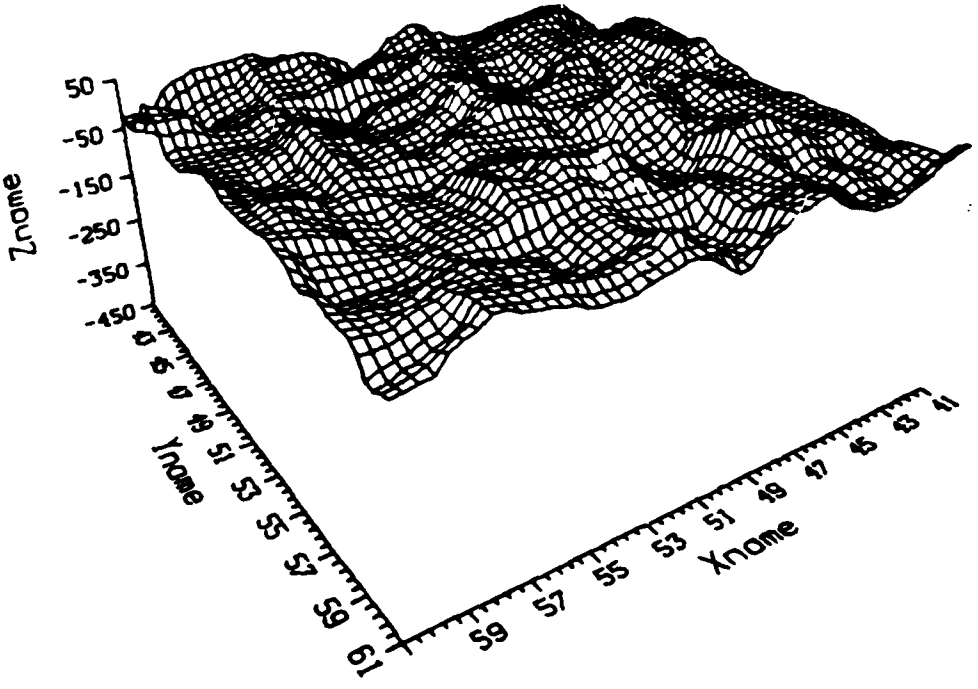

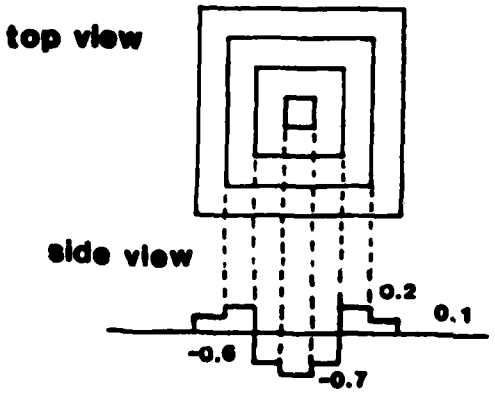

single impact plastic deformation profile

Figure 5 Computer simulation of surface morphology showing mogul formation after 10^6 random impacts each causing plastic deformation profile as shown , assuming that no material removal occurs.

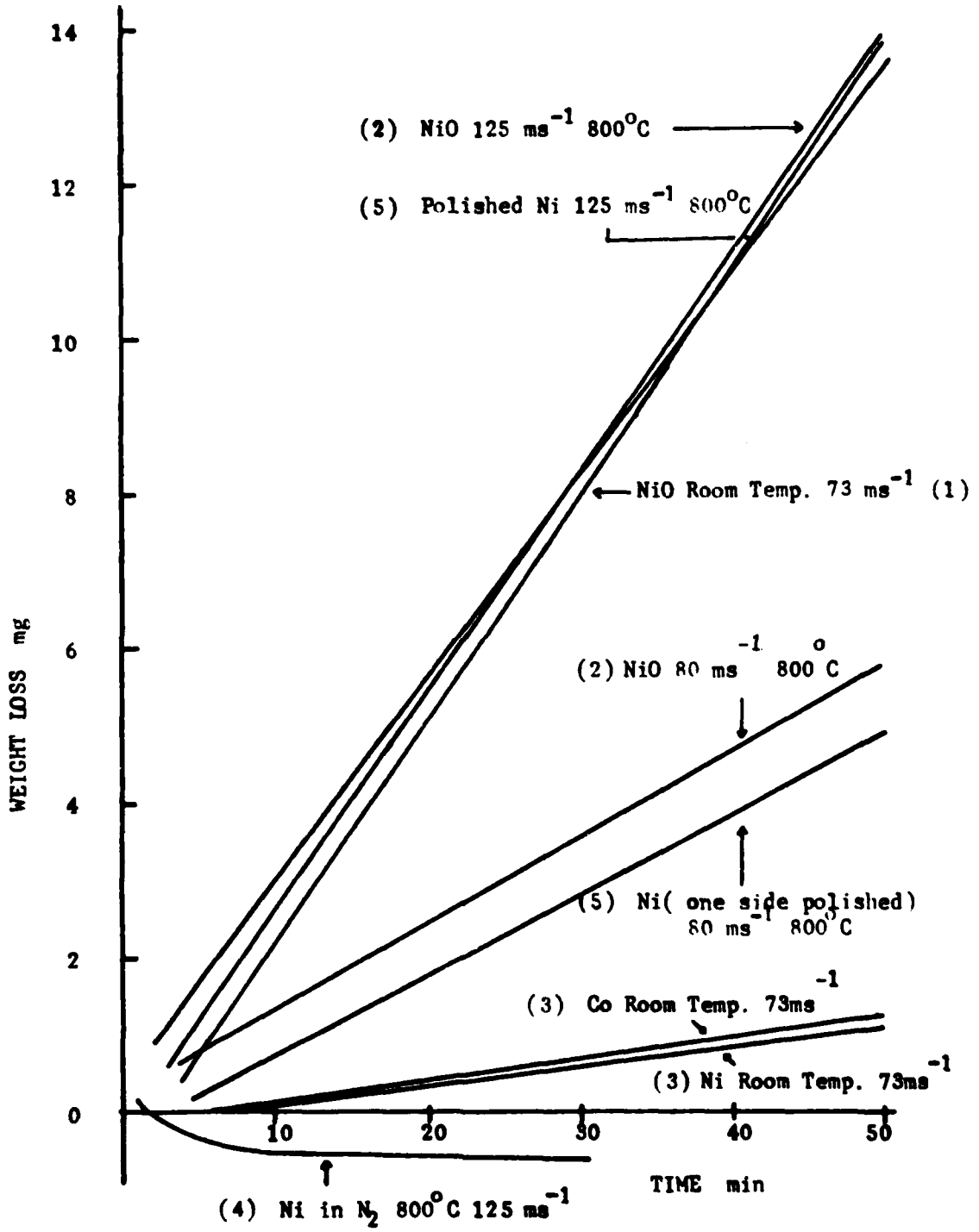

() refers to paragraph in report

FIGURE 6 Weight change with time for various erosion-oxidation condition.

Proceedings JIMIS-3 (1983) : High Temperature Corrosion
Transactions of the Japan Institute of Metals, Supplement

EROSION - CORROSION OF COATINGS AND SUPERALLOYS IN HIGH VELOCITY HOT GASES

C. T. KANG, S. L. CHANG, N. BIRKS AND F. S. PETTIT
Metallurgical and Materials Engineering Department
University of Pittsburgh, Pittsburgh, PA U.S.A.

Particle induced erosion of alloys at low (∿ ambient) temperatures and the corrosion of alloys at elevated temperatures in a wide variety of environments have been studied rather extensively. The effects of high velocity hot gases on corrosion of alloys have also been studied but to a more limited extent. On the other hand the degradation of alloys by combined erosion-corrosion in high velocity hot gases has not been studied in great detail. In this paper the erosion of alloys at ambient temperatures and the high temperature corrosion of alloys is briefly reviewed and then the combined erosion-corrosion of superalloys and coatings by hot gases is examined. It is shown that erosion-corrosion of alloys may occur by different mechanisms. When the particle energy is very large erosion can predominate to the extent that evidence of the corrosion process is extremely difficult to detect on the surfaces of alloys. Conversely, when the particle energy is low the effects of the erosion process can be neglected compared to the corrosion process. For some particle energies and corrosion rates interaction of the two processes can occur. Various types of interaction between erosion and corrosion processes are described.

INTRODUCTION

When structural alloys or coatings on such alloys are used at elevated temperatures in flowing gases conditions can be encountered where both corrosion processes (i.e. oxidation, mixed gas attack, hot corrosion) and erosion processes may take place concomitantly. It is therefore necessary to examine the mechanisms by which corrosion and erosion may take place concomitantly. In discussing combined corrosion-erosion a great range of conditions probably should be examined for a detailed understanding. At present the level of knowledge of corrosion-erosion processes is not sufficient to permit a totally general discussion. It therefore is appropriate to examine corrosion-erosion interactions under conditions similar to those which exist in some industrial applications. A reasonable choice is a gas turbine where materials can be exposed to elevated temperatures, high velocity gases containing particulate matter, and other environmental conditions that can cause oxidation, mixed gas attack and hot corrosion. While polymers as well as ceramics are used in gas turbines along with metallic alloys, this paper will consider only metallic systems. The two sections of a gas turbine in which conditions may be suitable for combined erosion-corrosion are the high pressure compressor and high pressure turbine. In the compressor the temperatures are often not high enough to cause substantial corrosion and alloys, especially coatings alloys, can be designed by considering only the erosion problem. In the high pressure turbine section very severe corrosion of alloys and coatings usually occurs, the presence of conditions producing erosion therefore represents a very

formidable problem. In practice when conditions causing combined corrosion-erosion are present in turbine sections a favored solution is to remove the particles from the gas stream through some sort of design change. Nevertheless, these conditions, when present, do represent conditions that can cause combined corrosion-erosion, and therefore they will be used in this paper as the basis for examining the interaction between corrosion and erosion.

In the following sections of this paper a very brief summary of metallic erosion will be presented followed by a concise description of the types of corrosion that can be observed in the high pressure turbine sections of gas trubines. Examples of combined corrosion-erosion will then be presented and discussed. These results will be used to begin to develop a map with which the different corrosion-erosion mechanisms can be compared and the factors important to transition from one mechanism to another can be identified.

EROSION OF METALLIC ALLOYS

The characteristic response of metals to erosive media as a function of time usually involves an incubation period during which very little erosion is evident, a period over which erosion is taking place at an increasing rate, and a period where the erosion rate is a maximum and approximately independent of time as indicated in Figure 1.

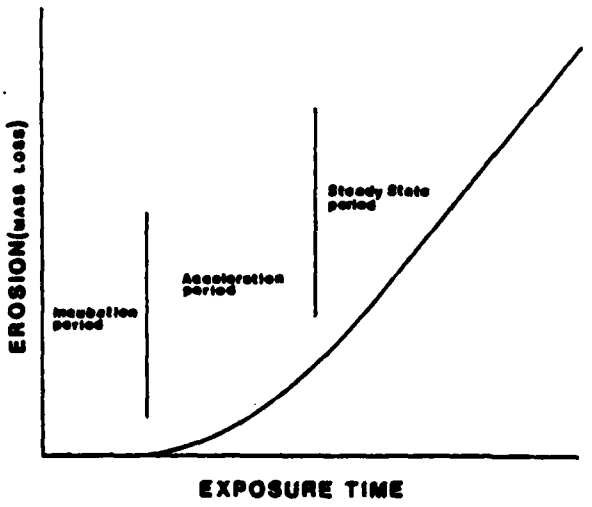

Figure 1. Erosion as a function of time of exposure.

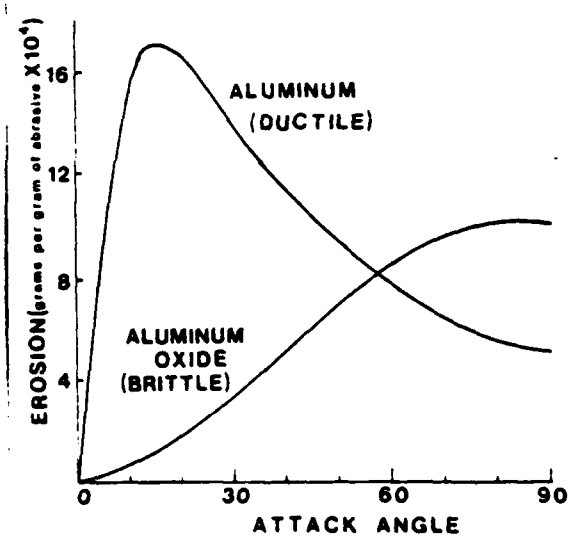

Figure 2. Erosion as a function of angle of impingement for aluminum and high-density aluminum oxide.

Most experimental erosion data are presented as the ratio of the mass of material removed to the mass of the impacting particles (gm/gm of abrasive) for a fixed exposure time increment where the exposure time corresponds to times at which the erosion rate is independent of time. Two types of response of materials to multiple solid impacts have been observed. One is a ductile response generally associated with metals and the other is a brittle response associated with

glasses or ceramics. The general form of the mass removal rate as a function of the angle of attack for each response is shown in Figure 2.

A number of theories have evolved to account for the erosion of materials. These models usually deal with ductile and brittle erosion separately. Rather complete descriptions of previous erosion research is available in review papers [1-3]. In this paper only the salient features of the current level of knowledge of erosion processes will be presented.

A common feature of many of the theories concerned with ductile materials is the application of a constant flow stress to represent material behavior. Finnie [4,5] treated the erosion of ductile materials as a gouging action similar to a tool cutting mechanism by using equations of motion for the abrasive particles. Bitter [6,7] divided the erosion process into a cutting wear mode (similar to Finnie's analysis) and a simultaneously occurring deformation wear mode. Bitter's model yields a relation between erosion rate and impingement angle which closely follows experimental data whereas the cutting wear model agrees with experimental data only at angles less than 45° unless empirical factors are used to account for roughening of the specimen surface. Bitter's model recognized that cutting wear does not occur at high impingement angles but it did not define the mechanisms by which material was removed by the deformation wear mode. Adjustable parameters with no assigned physical meaning were determined from measured data and used to account for the deformation wear mode. Hutchings and Winter [9-10] used optical microscopy and high speed photography to characterize the impact event. It was concluded that material removal can occur by plowing deformation or by two types of cutting deformation.

Mamoun [11] developed an expression for the erosion of a ductile target based on an erosion mechanism. He assumed that surface degradation could occur through a mechanism resembling fatigue as multiple particles impact the surface of a material. Particulate erosion in many ways is similar to wear and Jahannir [12] has extended delamination theories developed to account for wear [13] to the case of particle erosion. The use of a delamination theory is similar to Mamoun's approach in that it does not presuppose that each instance of particle impact results in material loss, but postulates a mechanism for accumulating damage which eventually leads to material removal. Levy and Bellman [14] have observed that plastic deformation within the impacted surface leads to the formation of platelets similar to those documented for delamination wear [13]. They propose that such platelets, once formed, are quickly detached upon subsequent particulate impacts. Follansbee [15] has also observed platelet formation during erosion and has developed an erosion model based upon a fatigue fracture failure eriterion.

In summary, the erosion of metals can consist of discrete, isolated impact craters, Figure 3a, or more uniformly eroded surfaces, Figure 3b. The uniformly eroded surfaces are common to erosion produced by multiple particle impacts and, as such, consist of materials removal processes involving accumulative deformation.

The mechanisms by which the accumulative deformation results in material removal are not well defined and probably are affected by numerous factors related to the elastic and plastic deformation of metals. It is also known that heat is generated in the specimen and the particle on impact but the effect of this on erosion mechanisms has not been established.

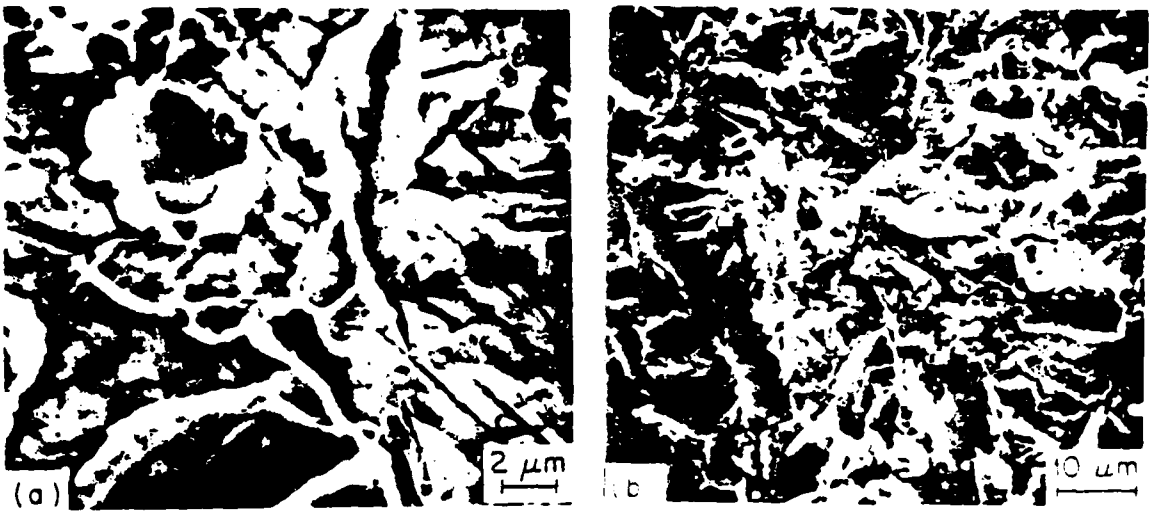

Figure 3. (a) Erosion impact craters on steel surface [16].
(b) AISI 310 steel surface after erosion at 25°C at 40 m/s [17].

In discussing the erosion-corrosion of metallic alloys it is also necessary to consider the erosion of ceramics since the corrosion products formed upon metallic alloys usually consist of some ceramics. Erosion of ceramics is usually viewed as a brittle process where material removal occurs mainly by chipping, Figure 4. A more modern view of ceramic erosion is based on the concept that the chipping process may consist of two regimes of cracking, namely, an elastic response regime and a plastic response regime [18]. Several types of fracture have been observed in the elastic regime, from single cone (Hertzian) cracks [19-21] to arrays of short circumferential surface cracks [18]. Material removal occurs by the interaction of these cracks, but the details of the process are complex and, as yet, poorly defined. It is evident that the fracture threshold will depend on specimen properties such as the surface flaw size distribution, the fracture toughness and the elastic wave speed. In the case of the plastic response both radial and laterial cracks are induced. The problem is an elastic-plastic one, and the hardness and the fracture toughness are the prime material parameters that control the extent of the fracture and consequently the erosion. The mechanism of material removal consists of chip formation which occurs due to the subsurface network of laterial cracks.

HIGH TEMPERATURE CORROSION OF METALLIC ALLOYS

A great number of high temperature corrosion processes could be considered when discussing corrosion in preparation for a discussion of combined erosion-corrosion. In practice, however, the systems of most interest are those which are relatively resistant to degradation, and consequently only corrosion resistant systems will be considered in this paper. In order for an alloy to be resistant to high temperature corrosion, the alloy must not react with the environment in which it is exposed (immunity) or, the product formed as a

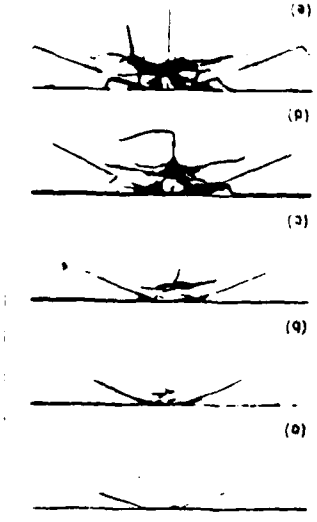

Figure 4. Photographs showing sequence of fracture damage when a sphere is pressed against a glass surface [18].

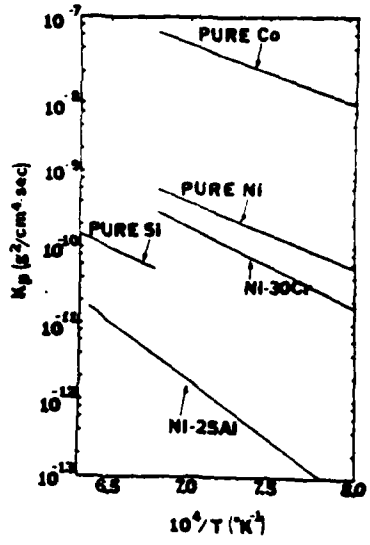

Figure 5. Temperature dependence of the parabolic rate constants for the growth various oxide barriers on metals and alloys (CoO on Co, NiO on Ni, SiO_2 on Si, Cr_2O_3 on Ni-30% Cr, α-Al_2O_3 on Ni-25% Al). The oxidizing environments for the data presented were 0.1 atm. oxygen for Ni, Ni-30Cr and Ni -25 Al; 0.125 atm. oxygen for Co and 1 atm. oxygen for Si.

result of reaction must inhibit subsequent reaction between the environment and the alloy [22,23] (passivation). Very few practical alloys posses both immunity to corrosive environments and desirable physical properties, hence virtually all the alloys encountered in practice achieve resistance to corrosion by passivation.

In most of the environments in which engineering alloys are used oxygen is very often present. Oxidation of alloys is therefore a very important form of high temperature corrosion. Other reactants in addition to oxygen however can be present and corrosion of alloys concomitantly by a number of reactants (mixed gas attack) is an important form of high temperature degradation. While gaseous induced degradation of alloys is the principal means of high temperature corrosion, deposits can be formed on alloys during use which may significantly affect the gas-induced corrosion process. Deposit modified high temperature corrosion is called hot corrosion and is an important means of alloy degradation especially in the case of materials used in gas turbine engines. In summary, the important forms of high temperature degradation of corrosion resistant systems are oxidation, mixed gas attack and hot corrosion.

When an alloy is exposed to oxygen at elevated temperatures the type of oxide barrier which is formed upon the alloy surface is determined by the composition of the alloy. The most effective oxide barriers to inhibit attack are Al_2O_3, Cr_2O_3 and SiO_2 as can be seen by comparing rate constants for the growth of these oxides, Figure 5.

Alloys possessing resistance to high temperatue corrosion therefore usually contain sufficient concentrations of aluminum, chromium or silicon such that oxides of these elements can be formed as continuous layers over the alloys' surfaces via selective oxidation. Factors which affect the selective oxidation of such elements have been discussed in previous papers [22,23].

Even though continuous and protective barriers of oxides such as Al_2O_3, Cr_2O_3 or SiO_2 can be formed on alloys via selective oxidation, as the alloys are continually exposed to the oxidizing environment in service the barrier becomes damaged. A principal means of damage occurs through thermally induced stresses that cause cracking and spalling of the protective oxide barriers. Cracking and spalling of the oxide scale followed by development of new oxide barriers depletes the alloy of the elements which are to be selectively oxidized. Hence, eventually the alloy will become so severely depleted of the element relied upon for selective oxidation that it will not be possible for the desired oxide to be formed as a continuous layer over the surface of the alloy and a less protective scale will begin to be formed. The degradation sequence of alloys in oxygen therefore consists of the development of the most thermodynamically stable oxides and then less stable oxides as the alloy becomes degraded. In the case of corrosion resistant alloys the more stable oxides also provide the most protection, hence, as the less stable oxides begin to form, the oxidation resistance of the alloy begins to decrease as illustrated by the data presented in Figure 6.

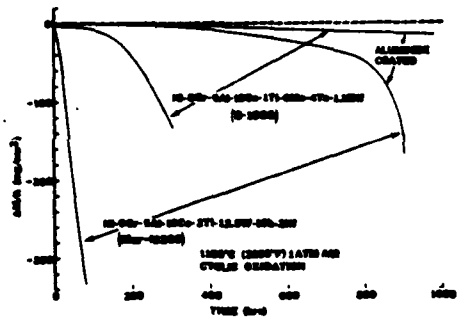

Figure 6. Weight change versus time data for the cyclic oxidation of two nickel-base superalloys and these two alloys coated using a diffusion aluminizing treatment. The degradation of these alloys consists of two stages. An initial stage of less severe attack (not evident on one of the uncoated alloys for the time scale used) and a subsequent stage of more rapid attack.

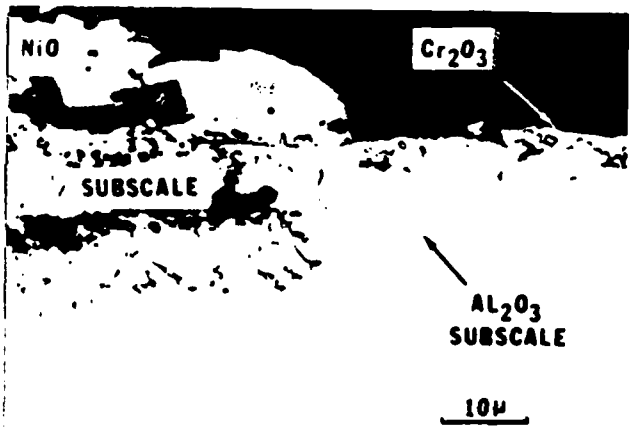

Figure 7. Nonuniform oxidation morphology developed on Ni-10Cr-1Al. After 20 hr. of oxidation of 0.1 atm. of oxygen at 1000°C. This type of oxide scale morphology frequently develops on alloys during cyclic oxidation testing as less protective oxides become stable.

This degradation sequence is followed for both structural alloys as well as coatings on such alloys. Since the coating alloys are designed for resistance to oxidation, it takes a longer time for the less protective oxides to be formed as can be seen upon comparing data for uncoated and coated alloys in Figure 6. In Figure 7 a photograph is presented which shows less protective nickel oxide being formed on an alloy which relies upon the development of a Cr_2O_3 scale for oxidation resistance.

In the case of mixed gas attack the most corrosion resistant systems are those upon which barriers of Al_2O_3, Cr_2O_3 or SiO_2 are formed. Many mixed gas environments contain sufficient oxygen for these oxide scales to be formed. When such alloys are used the degradation sequence described previously is followed but when the most protective oxide barrier can no longer be formed corrosion products involving the other reactants in the gas phase are formed as illustrated in Figure 8.

In the case of hot corrosion attack, the degradation sequence also involves formation of the most protective oxide barriers with the eventual formation of less protective corrosion product phases as indicated in Figure 9.

The hot corrosion process may involve a number of different mechanisms by which the protective oxide barrier is destroyed, depending upon the conditions causing the hot corrosion attack. It is sufficient in this paper to indicate that resistance to hot corrosion attack is obtained via selective oxide barrier formation and that the hot corrosion conditions usually decrease the time period over which the alloy is capable of resisting attack by repeatedly reforming the desired protective oxide barrier.

In this discussion on high temperature corrosion resistant systems, the importance of the degradation sequence has been emphasized. In particular, in the case of oxidation, mixed gas attack or hot corrosion the degradation sequence consists of an initial stage during which oxide reaction product barriers are formed via selective oxidation and protect the alloys from the environmentally induced attack. Eventually in this sequence lesser protective products begin to be formed and the alloys can be considered to be no longer resistant to the environment. It is worth emphasizing that the adherence of the oxide barrier is also another rather critical factor determining how long the alloy will be capable of sustaining the most protective oxide barrier on its surface. Oxygen active elements and/or inert oxide particles can be used to significantly improve the capability of oxide scales to resist cracking and spalling from the surfaces of alloys [24-26). The mechanism by which such oxides or oxygen active elements improve the scale adherence is not known and a number of different mechanisms have been proposed.

EROSION - CORROSION OF ALLOYS

To illustrate some of the interactions that have been observed for combined erosion-corrosion, data obtained from specimens exposed at 870°C to α-Al_2O_3 particles (0.3, 2.5 and 20 μm average particle size) with velocities of about 190 m/s will be used [27]. The corrosion conditions consisted essentially of

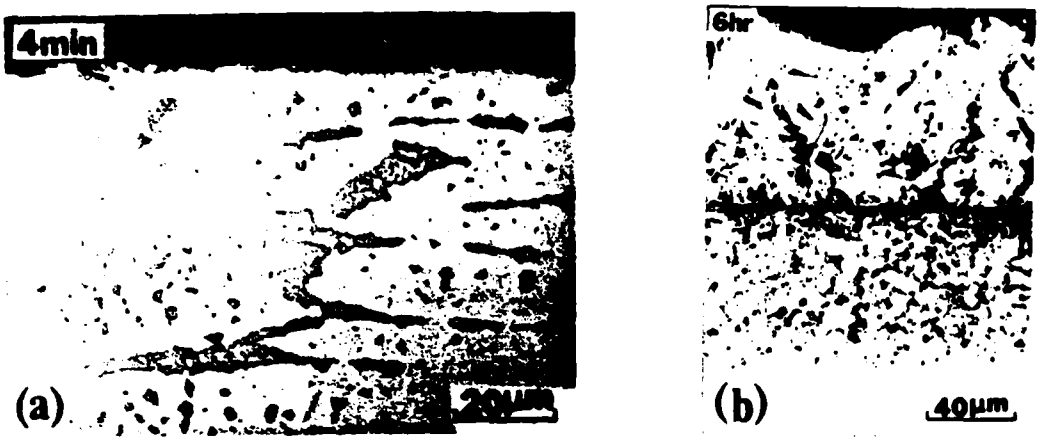

Figure 8. Photomicrographs showing the reaction products formed on Co-25Cr-6Al during exposure to a $H_2S/H_2/H_2O$ gas mixture with $P_{S_2} = 10^{-5.35}$ at 900°C. (a) After 4 min. of exposure the reaction product is a very thin Al_2O_3 - rich scale which is not evident and the alloy substrate exhibits no features indicative of degradation. (b) After 6 hr. a substantial reaction product has been formed which is composed of sulfides above and below an oxide scale (arrows).

oxidation in air or hot corrosion in air induced by deposition of Na_2SO_4. Both superalloy specimens (i.e. X-40, IN738) and superalloy specimens with coatings (diffusion aluminide or MCrAlY) will be considered.

Exposure of specimens to oxidizing gases containing about 130 ppm of 20μm particles resulted in very severe degradation of all the alloys. For example, weight losses of about 200 mg/cm^2 were observed after about 30 hours of exposure. A significant difference between the α-Al_2O_3 formers (coated alloys) and Cr_2O_3 - formers (uncoated alloys) was not apparent. The surfaces of a typical specimen after preparation, after oxidation, and after oxidation-erosion are presented in Figure 10. Detailed examination of the surfaces of the specimens exposed to oxidation-erosion showed that as the angle of impingement was decreased the impact craters became more elongated, Figures 11a and 11b. These results are similar to those observed for erosion of metals at room temperature. The surfaces of all the specimens exposed to the oxidation-erosion conditions did not appear to contain any oxidation products. It was determined, however, that all of the surfaces were covered with very thin layers of oxide scales, Figure 11c. The results obtained with 20 μm particles show that the erosive component is very large compared to the oxidation component. Oxidation is occurring. The removal of metal due to cutting and deformation is so rapid, however, that the amount of oxidation on freshly exposed surfaces is negligible. For such conditions it appears that the oxidation process can be neglected and the metal loss can be assumed to be determined solely by the erosion process.

Oxidation tests performed under conditions similar to those described in the preceding paragraph but with 300 ppm of 2.5 μm α-Al_2O_3 particles rather than

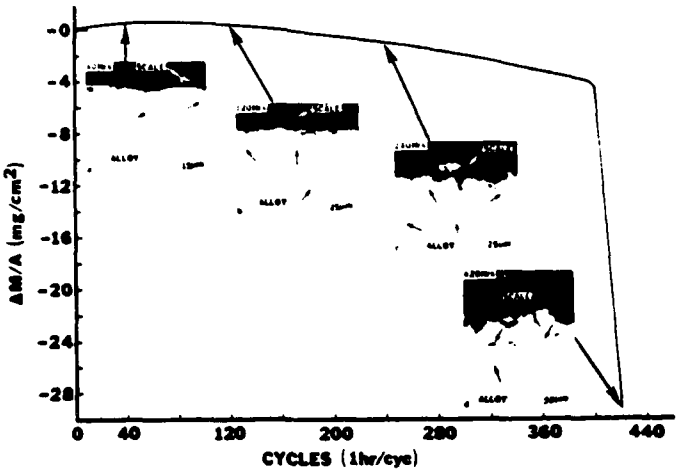

Figure 9. Weight change versus time data and corresponding microstructural features for the cyclic hot corrosion of Na_2SO_4-coated (5 mg/cm^2 applied every 20 hours.) Ni-30Cr-4Al in air at 900°C. The amount of sulfide particles (small black arrows) increases until the oxidation of the sulfide phases significantly affects the rate of attack.

20 μm particles caused a significant amount of alloy degradation. It was substantially less than that observed with 20 μm particles and it appeared to be influenced by the type of oxide scale which was formed on the surface of the alloys. For example after 30 hours of exposure, the Cr_2O_3 - formers lost about 60 mg/cm^2 compared to about 30 mg/cm^2 for the Al_2O_3 - formers. The surface of a typical specimen is shown in Figure 12. The surface features did not appear to be markedly dependent upon the angle of impingement. The features observed upon the surfaces of specimens appear to consist of platlets and may be similar to those observed on some metals during erosion at ambient temperatures [14]. The observation that the weight-losses of the Cr_2O_3 - formers were significantly larger than those of the Al_2O_3-formers indicates that the Al_2O_3 scales had some affect on the combined oxidation - erosion process. It has been determined that Cr_2O_3 scales do form volatile products (i.e. CrO_3) in gases at high velocities (e.g. $\sim$ 200 m/s) even at temperatures as low as 870°C [27]. It appears that in the case of the Al_2O_3 - formers the oxide scale was thick enough to affect the erosion process. Results obtained in other investigations [28,29] also suggest that oxidation products can inhibit erosion processes.

Oxidation-erosion experiments performed with 0.3 μm Al_2O_3 particles at 870°C did not produce any evidence of erosion on either the Al_2O_3-formers nor the Cr_2O_3 - formers. The results were similar to those obtained without any particles. These observations show that there are conditions where the erosion component is negligible compared to the corrosion component.

Specimens which were exposed to combined erosion-hot corrosion conditions using Na_2SO_4 to induce hot corrosion and 2 μm Al_2O_3 particles to cause erosion were very severly degraded. Results obtained for a coated cylindrical

Figure 10. Scanning electron micrographs of replicas from X-40. (a) pre-test condition (600 grit polish), (b) after 4.5 hours of oxidation at 870°C, (c) after 4.5 hours of oxidation - erosion at 870°C (130 ppm, 20 μm α-Al_2O_3 90° impingement angle.)

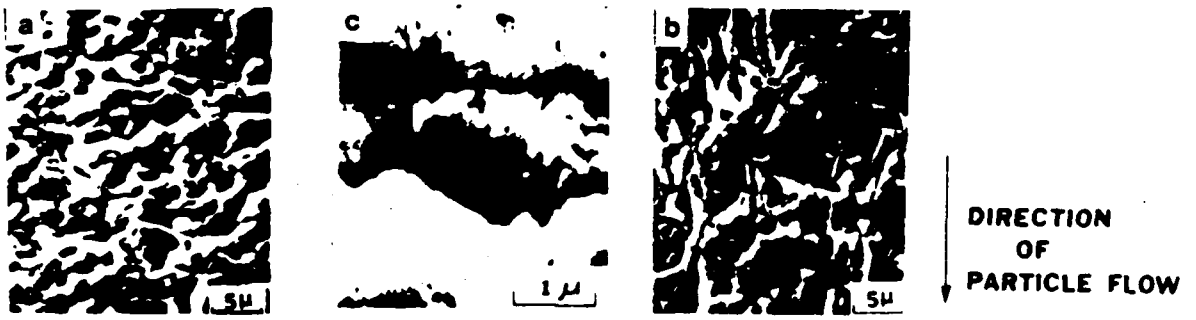

Figure 11. Scanning micrographs illustrating surface features developed on IN738 after 20 hrs. of oxidation-erosion testing at 871°C using 20 μm α-Al_2O_3 at a loading of 130 ppm. At impact angles of 90°, (a) craters having raised edges are evident. As the angle of impact is decreased, the impact craters become elongated and at 5°, (b) appear as micromachining markings. Features were observed on the impact craters, arrows (c) that indicated the surfaces of the specimens were covered with a very thin layer of oxide.

specimen are presented in Figures 13. The leading edge of this specimen was exposed to erosion-hot corrosion conditions whereas the trailing edge was exposed to only the hot corrosion component. At some angles of particle impingement the coating has been completely consumed, Figure 13d, whereas on the trailing edge the coating has undergone very little degradation, Figure 13e. The weight losses of the specimens exposed to the combined erosion-hot corrosion

conditions were substantially greater than the sum of the weight losses for hot corrosion with no erosion and erosion-oxidation. These results indicate that the erosion and hot corrosion processes are interacting such that their combined effect is greater than the sum of the two processes acting independently. In this paper it is not possible to discuss this observed interaction in great detail. As shown in Figure 14, it was observed that the specimens subjected to combined erosion-hot corrosion had less corrosion product on their surfaces than those exposed only to the hot corrosion conditons. It appears that the particles removed some of the porous oxide. This caused the hot corrosion component to be increased since the Na_2SO_4 was not retained in the porous scale and hence the Na_2SO_4 more effectively covered the alloy surface. As shown in Figure 15, the hot corrosion component caused portions of the alloys to be undercut. It is believed that such a condition permitted the particles to more efficiently remove metal from the surface of the alloy.

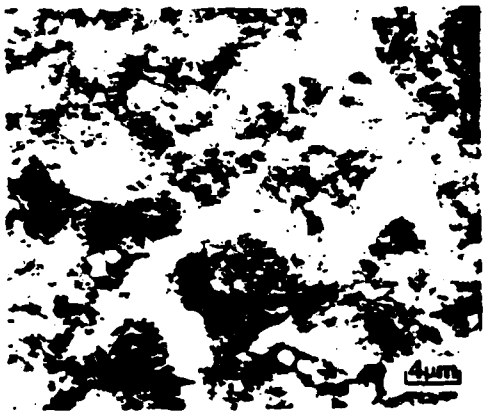

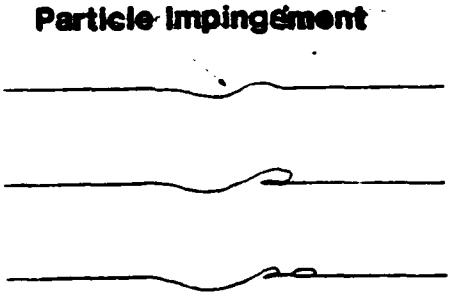

Figure 12. Surface features and schematic diagram of proposed mechanism of metal removal by 2 μm Al_2O_3 abrasive. Features are typical of high and intermediate impingement angles, the small particles on the surface possible becoming detached by a mechanism of the type illustrated in the sketch.

The results that have been presented on combined erosion-corrosion have not been very extensive. These results are sufficient however to illustrate some of the types of interactions which are believed to be important in regards to combined erosion-corrosion, in particular.

- When the relative magnitude of one of the erosive and corrosive components is very small compared to the other, the smaller of the two components does not exert a significant effect on the degradation process.

- When the magnitude of the components are comparible, interactions between erosion and corrosion can be expected, the following interactions have been observed.

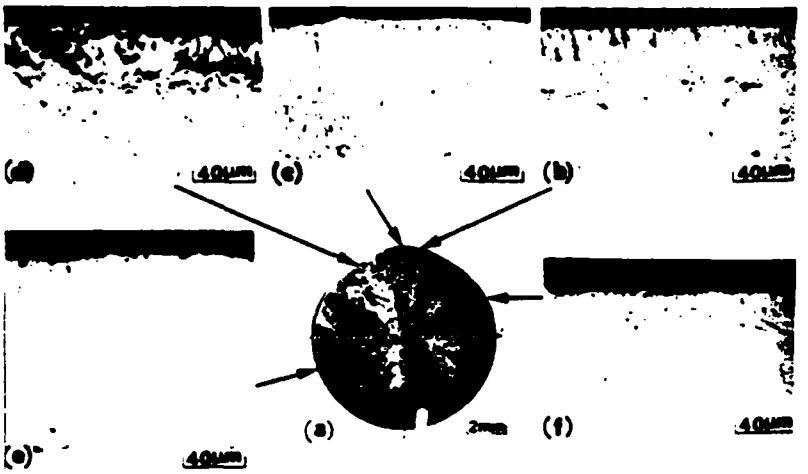

Figure 13. Typical microstructures that developed during exposure of a CoCrAlY coating on IN738 to 28 hours. of erosion-hot corrosion (2.5 μm Al_2O_3, 0.05 mg/cm^2 hr. of Na_2SO_4-22% K_2SO_4) at 871°C.

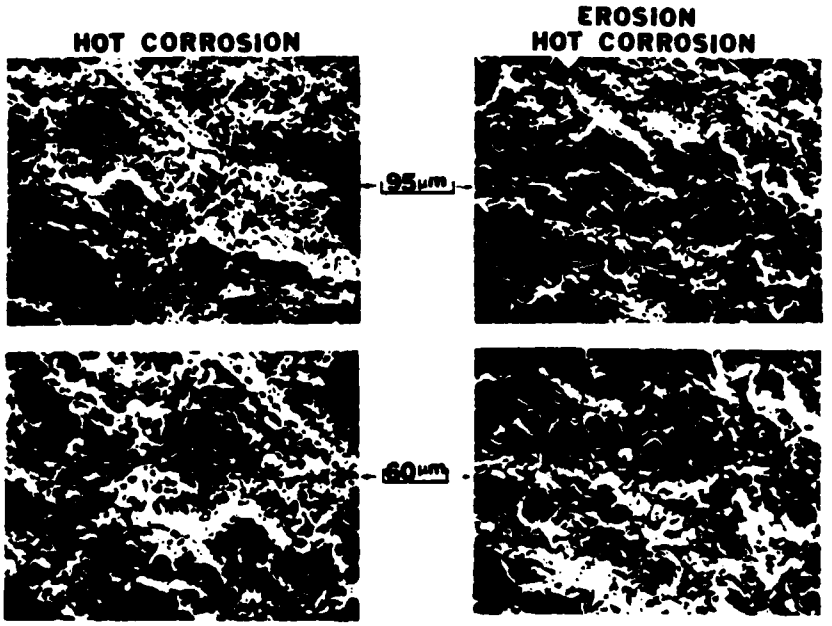

Figure 14. Scanning micrographs showing features of the oxide scales formed on IN738 after exposure to the hot corrosion test (0.05 mg/cm^2-hr. Na_2SO_4-22% K_2SO_4) and the erosion-hot corrosion test (0.05 gm/cm^2-hr Na_2SO_4- 22% K_2SO_4 and 300 ppm 2.5 μm α-Al_2O_3 particles) at 871°C. The arrows identify the same areas at progressively higher magnifications. It is apparent that the erosive component has removed much of the porous oxide that is normally developed during hot corrosion attack.

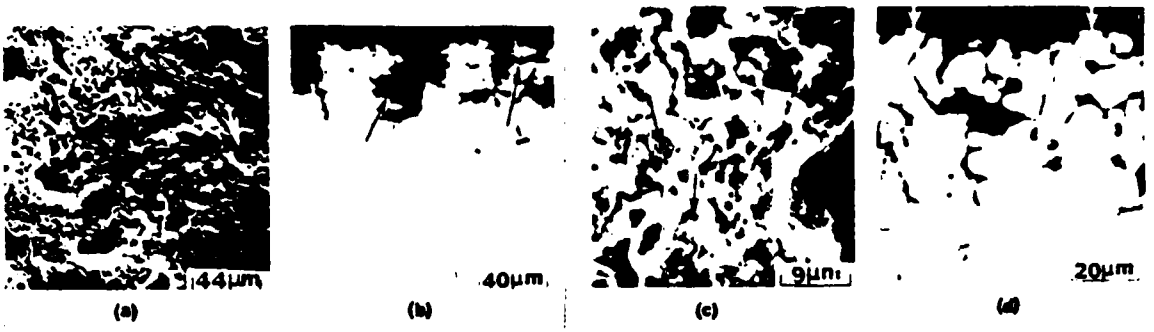

Figure 15. Photographs of IN738 after 28 hours exposure to erosion hot corrosion conditions at 870°C to illustrate features of the erosion-hot corrosion process; large craters on the surface, arrows (a) are believed to occur because of dislodgement of oxide and alloy, arrows (b) Numerous areas of the surface are covered with oxide, black arrows (c) but exposed alloy or alloy covered with much thinner oxide is also evident, white arrows (c) and (d).

- corrosion inhibited erosion
- corrosion enhanced erosion
- erosion enhanced corrosion

For instance relatively large particles (20 μm) impacting at high velocities would be expected to cause vigorous erosion compared to which the oxidation component is small, particularly if the oxide forms only slowly, e.g. Al_2O_3. If the same conditions are maintained but the particle size is decreased to, say, 2 μm, the impact energy rate will be decreased and the oxide formed might begin to inhibit the erosion process, possibly depending on the nature of the oxide formed. Alternatively the impacts may crack the scale leading to enhanced oxidation.

At extremely small particles sizes (0.3 μm) the erosion component may even become negligible compared with oxidation degradation, in fact these particles may deposit on the existing growing oxide scale.

The boundaries at which these changes in behavior occur will also depend on the scale growth rate.

It may be possible to represent these complex interactions by using a diagram, as sketched in Figure 16, using particle energy and scale growth rate as coordinates. On Figure 16 are delineated areas of degradation by pure erosion, oxidation inhibited erosion, erosion enhanced oxidation and pure oxidation.

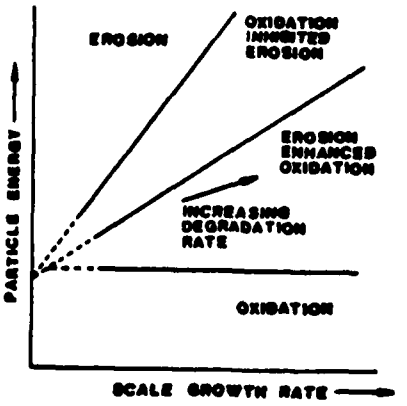

Figure 16. Schematic diagram to illustrate the possible relationship between different regimes of materials degradation as a function of particles energy and scale growth rate for a combined erosion-oxidation process.

CONCLUDING REMARKS

The combined erosion-corrosion of alloys in high-velocity, hot, gases has not been studied in great detail. In order to understand this type of alloy degradation it is necessary to utilize the knowledge which is available on ambient temperature erosion and high temperatue corrosion and apply it to investigations of combined erosion-corrosion. The results which are available indicate that, depending upon the magnitude of the erosive and corrosive components, different types of degradation modes are important. It is necessary to interrelate these degradation modes as a function of the intensity of the erosive and corrosive components.

ACKNOWLEDGEMENT

The authors wish to acknowledge the support of the Army Research Office (contract number DAAG-29-81-K-0027) in preparation of this paper.

REFERENCES

[1] Erosion Control In Energy Systems, National Materials Advisory Board, National Academy of Sciences, 1977, Report No. NMAB-334.

[2] W. F. Adler: Assessment of the State of Knowledge Pertaining to Solid Particle Erosion, Tech. Report, Effects Technology, Inc., 1979, NTIS, Report No. ETI-CR79-680.

[3] A. W. Ruff and S. M. Wiederhorn, Erosion by Solid Particle Impact; Treatise on Materials Science and Technology, Vol. 16, C. M. Preece, editor; Academic Press, New York, 1979.

[4] I. Finnie, Wear, 3(1960), 87.

[5] I. Finnie, A. Levy, D. H. McFadden, Fundamental Mechanisms of Erosive Wear of Ductile Materials by Solid Particles; Erosive: Prevention and Useful Applications, W. F. Adler, editor, ASTM STP 664, 1977.

[6] J. G. A. Bitter, Wear, 6(1963), 5.

[7] J. G. A. Bitter, Wear, 6(1963), 169.

[8] I. M. Hutchings, R. E. Winter and J. E. Field, Proc. Royal Society Landon, A 348 (1976), 379.

[9] R. E. Winter and I. M. Hutchings, Wear, 34 (1975), 141.

[10] R. E. Winter and I. M. Hutchings, Wear, 29 (1974), 181.

[11] M. M. Mamoun, Materials Science Division Coal Technology Third Quarterly Report, Tech. Report ANL-75-XX3, Argonne National Laboratory, 1975, Appendix: Analytical Models For the Erosive-Corrosive Wear Process.

[12] S. Jahanmir, Wear (1980), 309.

[13] N. P. Suh, Wear, 44 (1977), 1.

[14] R. Bellman, Jr. and A. Levy, Erosion Mechanism in Ductile Metals, Tech. Report, Lawrence Berkeley Laboratory, LBL-10289, 1980.

[15] P. S. Follansbee, Mechanisms of Erosive Wear of Ductile Metals Due to the Low Velocity, Normal Incidence, Impact of Spherical Particles, Ph.D. Thesis, Carnegie-Mellon University, 1981, Pittsburgh, PA.

[16] L. K. Ives, J. P. Young and A. W. Ruff, Nat. Bur. Stds., SP 468, (1977) 145.

[17] L. K. Ives, J. Eng. Mater. Tech. Trans. ASME 99(1977), 126.

[18] A. G. Evans and T. R. Wilshaw, J. Mater, Sci., 12(1977), 97.

[19] G. L. Sheldon and I. Finnie, Trans. ASME, 88B(1966) 393.

[20] W. F. Adler, Analysis of Multiple Particle Impacts on Brittle Materials, AFML-TR-74-210, (1974).

[21] W. F. Adler, Erosion of Fused Silica by Glass Beads, Erosion, Wear and Interfaces with Corrosion, American Society for Testing and Materials, STP 567 (1974).

[22] F. S. Pettit, C. S. Giggins, J. A. Goebel and E. J. Felten, Oxidation and Hot Corrosion Resistance, Alloy and Microstructural Design, J. K. Tien and G. S. Ansell, editors; Academic Press, New York, 1976.

[23] F. S. Pettit and G. W. Goward, High Temperature Corrosion and Use of Coatings for Protection, Metallurgical Treatises, J. K. Tien and J. F. Elliott, editors, The Metallurgical Society of AIME, Warrendale, PA., 1981.

[24] J. K. Tien and F. S. Pettit, Met. Trans. 3(1972) 1587.

[25] F. H. Stott, G. C. Wood and J. G. Fountain, Oxid, Metals, 14(1980) 135.

[26] D. P. Whittle and J. Stringer, Phil. Trans. Roy Soc. Lond. 295(1980) 309.

[27] R. H. Barkalow, J. A. Goebel and F. S. Pettit, Materials Problems in Fluidized - Bed Combustion Systems, High-Temperature Erosion-Corrosion by High-Velocity (200 m/s) Particles, CS-1448, Research Project 979-4, Electric Power Research Institute, Palo Alto, CA., 1980.

[28] J. P. Young and A. W. Ruff, J. Eng. Mater. Tech. Trans. ASME 99 (1977) 121.

[29] N. A. Mikhailova, Zashch. Metall. 11 (1975) 641.